Accepted Manuscript

Bleeding and sedimentation of cement paste measured by hydrostatic pressure and Turbiscan

Y. Peng, R.A. Lauten, K. Reknes, S. Jacobsen

PII: S0958-9465(16)30791-0

DOI: 10.1016/j.cemconcomp.2016.11.013

Reference: CECO 2746

To appear in: *Cement and Concrete Composites*

Received Date: 18 January 2016

Revised Date: 23 November 2016

Accepted Date: 29 November 2016

Please cite this article as: Y. Peng, R.A. Lauten, K. Reknes, S. Jacobsen, Bleeding and sedimentation of cement paste measured by hydrostatic pressure and Turbiscan, *Cement and Concrete Composites* (2017), doi: 10.1016/j.cemconcomp.2016.11.013.

Bleeding and sedimentation of cement paste measured by hydrostatic pressure and Turbiscan

Y. Peng[1*], R. A. Lauten[2], K. Reknes[3], S. Jacobsen[1]

1. Norwegian University of Science and Technology
2. Borregaard AS
3. Skanska Norge AS

* Corresponding author, yapeng2007@hotmail.com, +47 45095716

Abstract

Sedimentation and bleeding of cement pastes with lignosulfonate were studied by visual observation, HYdroStatic Pressure Test (HYSPT) and Turbiscan measurements showing two bleeding stages: a fast initial phase followed by a phase with diminishing sedimentation rate. A turbid bleeding zone establishes during the fast bleeding phase and the top layer gradually becomes transparent in the diminishing phase within minutes or hours depending on admixture and solid fraction. The bleeding rates measured visually and by HYSPT in the first 2 hours are higher than the ones calculated by Kozeny-Carman Equation, whereas turbiscan shows lower rates. Both HYSPT and Turbiscan monitor the particle and fluid fluxes and thus describe bleeding from turbid to clear zone respectively by observing the density variation of bulk paste or the change in optical density of the surface region. Lignosulfonate reduces bleeding by improving particle dispersion to various degrees depending on types and dosages.

Key words: cement paste (D), admixture (D), bleeding (A), turbid

1. Introduction

Instability phenomena of cement paste and concrete occur due to density differences between the basic constituents spanning from water with density 1000 kg/m^3 to solids with density 2700-3150 kg/m^3. Generally, bleeding of cementitious materials is the sedimentation consequence of temporarily suspended particles. In 1939 Powers [1] concluded that the major factors controlling bleeding of cement paste and concrete are the water content and the surface area of the solids. He also explained that bleeding occurs in two stages: a period of fast constant rate followed by one with diminishing rate. The bleeding rate during the constant period can be assumed to follow general laws derived from

Darcy [2] and Poiseuille's law [3] of capillary flow [4] in a bed of fines and solid particles, leading to the Kozeny-Carman (K-C) Equation [5], as shown in Eq. (1). There, Q is the bleeding rate (m/s), ε is the paste porosity (m^3/m^3), k_c is the Carman constant (k_c=4.1 according to Powers [5]), μ is the viscosity of the fluid phase (Pa·s), g is the gravity acceleration (m/s^2), σ is the specific surface of the particles (m^2/m^3), ρ_s and ρ_f are the densities (kg/m^3) of the solid particles and fluid.

$$Q = \frac{\varepsilon^3}{1-\varepsilon} \cdot \frac{(\rho_s - \rho_f)g}{k_c \mu \sigma^2} \quad (1)$$

All of Powers research was based on visual observation on the movement of the interface between bleed water and segregated paste or concrete. However, novel research [6, 7] shows that the bleeding front is not always sharp in modern concrete mixes due to slow sedimentation of fine particles and a preference for higher contents of fine particles combined with use of chemical admixtures such as superplasticizers (SP) and Viscosity Modifying Agents. Daczko [8] also proposed that a mixture can be unstable even without clear bleeding. More recent research [9] on cement pastes with initial solid volume fractions 0.3~0.5 (corresponding to w/c=0.4~0.7) and varying powder content or admixtures addition show laminated bleeding zones with both clear bleeding layer and a soft turbid layer consisting of well dispersed fines. In-situ measurements of the w/c ratio by pipette [7] demonstrated substantial variation in the top surface zone. Therefore, the traditional term "bleeding" is about to lose its meaning for modern cement paste like in Self Compacting Concrete (SCC). This implicates that the properties of the hardened concrete at the surface can vary considerably from the bulk properties which may have large influence on both the durability and the surface quality.

For cement paste with high initial solid fraction, simple analysis of a single particle sinking in the fluid according to Stokes' Law [10] is no longer valid. Instead, multi-particle interactions must be taken into account. The presence of a large number of fine particles has four profound effects on the properties of cement paste. First, the motion of a single particle will be limited by the surrounding particles and thus the effective particle settling rate decreases. Secondly, an increasing volume fraction raises the viscosity and yield stress towards infinity. Thirdly, emergence of yield stress and associated percolated network also decreases the particle settling rate. Finally, the sum of inter-particle forces or

flocculation state influences the sedimentation process [7, 9]. In addition to the effect of solid fraction, the composition of solid phase and presence of admixtures will affect the settling. Furthermore, the reabsorption of bleeding water may also affect particle sedimentation and bleeding rate [10, 11, 12]. In [9] it was found that the Richardson-Zaki Equation (R-Z) [13] to some extent is applicable to describe the sedimentation in cement paste or filler modified matrix. It describes the empirical relation between Stokes terminal sinking velocity for a single particle and the effect of surrounding particles at arbitrary volume fractions (Φ). As multiple particles sink, various zones form. Kynch [15] first described the movement of particles between different zones. Fitch [16] later included compression of the sediment cake and suggested a relationship between the settling rate U_p, the flocculation tendency and solid concentration Φ. In this research, zone formation in cement pastes by sedimentation are defined as follows: bleeding water collected on the top followed by a homogeneous concentration zone, a variable concentrated zone and finally a sediment cake at the bottom, as illustrated in Fig. 1.

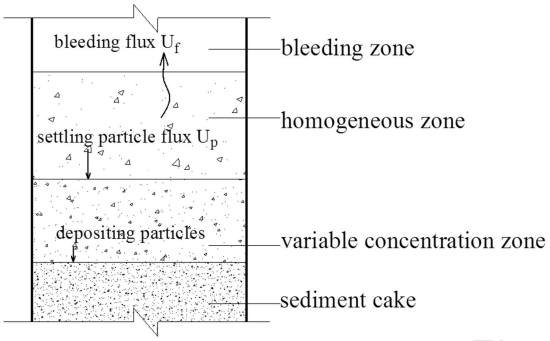

Fig. 1: Different zones in suspension during sedimentation

Traditional experimental methods to measure bleeding [17, 18, 19, 20, 21] rely on the measurement of visual bleeding depth or total bleeding and therefore cannot be used without a clear bleeding front. Microscopy or spectroscopy may be used to study the variation of concentration and the consequent bleeding, but the upper limit in solids fraction is only around 0.1. Therefore, the development of new test methods is important to investigate the bleeding of cement paste with normal solid fraction. The applicability and repeatability of HYSPT for fresh cement paste was explained in [7]. There is a reasonable correspondence between bleeding rate measured with pipette and calculated from hydrostatic pressure gradient. In the calculation of the bleeding rate from dP/dt, the pressure gradient at a specific depth, bleeding could be assumed to be a sharp front and a homogeneous zone beneath it

[7]. HYSPT also indicates the paste flocculation state which relies on that at a given initial Φ_0 better dispersed particles sink slower than flocculated ones. The bleeding depth was calculated according to Eq. (2), where P (h,t) is the detected pressure (Pa) at the height to paste surface h (m) and time t (s), h_b is the bleeding depth (m), Φ_0 is the initial solid fraction (in homogeneous zone Φ is assumed to be equal to Φ_0), ρ_p and ρ_f are respectively the mass densities of the particle and fluid (kg/m^3).

$$P(h,t) = \rho_f g h_b + [\rho_p \Phi_0 + \rho_f(1-\Phi_0)] \cdot g \cdot (h - h_b) \quad (2)$$

Time dependent turbidity measurement on the bleeding layer is the other method employed in this research to study sedimentation and formation of a bleeding layer. A Turbiscanner was used to measure the turbidity as a function of time for sedimenting cement paste. This apparatus has been used to detect sedimentation of dispersed or flocculated particles and the consequent bleeding of emulsions and suspensions, but rarely applied for cement paste. Meunier [22] first described it as a new concept to evaluate stability in concentrated colloidal dispersions. Later Meunier et al. [23, 24] and more recently Lemarchand et al. [25] applied it to analyze stability of emulsions or suspensions. The effect of polycarboxylate (PCE) superplasticizer on supernatant of suspensions was observed with Turbiscan in the research by Autier et al. [26], but the solid fractions of the suspensions are much lower than normal cement paste. Here we for the first time attempt to use the intensity variation of the transmitted light to investigate bleeding of cement paste with practical w/c between 0.4 and 0.7.

As mentioned, modern cement pastes often have a high content of fine particles and various admixtures which reduce the particle sedimentation rate and cause turbid bleeding above the denser bulk paste. Turbid bleeding is hard to observe by traditional bleeding test methods and often not addressed in research about bleeding phenomena. The scope of this work is to investigate the mechanism of bleeding, the development of a turbid bleeding zone and the effect of lignosulfonate (LS) representing a traditional plasticizer, on this process. For this purpose, sedimentation and bleeding of neat cement pastes with or without LS were measured by observing the variation in hydrostatic pressure of fresh paste as well as by optical scanning of the turbid bleeding zone by Turbiscan. Both methods follow the evolution from fresh homogeneous suspension to segregated paste with a combined clear-turbid bleeding zone and a dense sediment cake. In addition, the bleeding rates

measured with the two new methods are compared with those from traditional visual bleeding tests and the K-C Equation. Hopefully the research on the turbid bleeding and the application of new measurement methods can improve the understanding of how bleeding occurs in modern cement paste.

2. Materials and measurement methods

2.1. Materials

The recipes of the samples for all measurements are shown in Table 1. Four types of LS, described by a DP-number are applied with main characteristics shown in Table 2, where Mn is the number average molecular weight, Mw is the average molecular weight. All the LS dosages are solid dosage by cement weight (% sbwc).The cement used in this research is Norwegian standard Portland cement STD-CEM I with main chemical and physical characteristics shown in Table 3. Paste samples for Turbiscan experiments were prepared by weighing cement, water and LS into a beaker. The paste was stirred by an overhead mixer with a U-shaped impellor for three min at 200 rpm, kept at rest for five min followed by mixing at 200 rpm for two more min. Around 20 ml paste was filled into the Turbiscan vial with 2.5 cm diameter (filling height: 4.5~5 cm) and placed into the instrument. The Turbiscan measurements normally commenced around 15 min after first contact between cement and water. Around 3 liters of cement paste was mixed separately in a 5 liter Hobart mixer for HYSPT and visual bleeding tests with the following mixing procedure: the dry cement was mixed at low speed for 1 min; water and SP was added simultaneously and mixed for 2 min at lower speed 136 rpm; then changed to middle speed 281 rpm, continued mixing for 1 min, waited for 5 min while using spatula and hand to check for agglomerates; at last mixed the paste at middle speed for 1 min. After mixing, the samples were filled to the required heights in two cylinders for both tests. The top of the cylinders was covered and both tests started around 10 min after water addition. The duration of all experiments, HYSPT, visual bleeding and Turbiscan were 4 h.

Table 1: The recipes of all the samples

No.	Sample code	w/c	solid fraction Φ	lign. type	dosage (sbwc)
1	wc0.4	0.4	0.442	/	/
2	wc0.5	0.5	0.388		
3	wc0.6	0.6	0.346		
4	wc0.7	0.7	0.312		
5	23-wc0.4p0.3	0.4	0.442	DP1523	0.3
6	23-wc0.5p0.3	0.5	0.388		
7	23-wc0.6p0.3	0.6	0.346		
8	23-wc0.5p0.2	0.5	0.388	DP1523	0.2
9	23-wc0.5p0.5				0.5
10	24-wc0.4p0.3	0.4	0.442	DP1524	0.3
11	24-wc0.5p0.3	0.5	0.388		
12	24-wc0.6p0.3	0.6	0.346		
13	24-wc0.4p0.5	0.4	0.442	DP1524	0.5
14	24-wc0.5p0.5	0.5	0.388		
15	24-wc0.4p0.8	0.4	0.442	DP1524	0.8
16	24-wc0.5p0.8	0.5	0.388		
17	24-wc0.6p0.8	0.6	0.346		
18	25-wc0.4p0.3	0.4	0.442	DP1525	0.3
19	25-wc0.5p0.3	0.5	0.388		
20	25-wc0.6p0.3	0.6	0.346		
21	25-wc0.5p0.2	0.5	0.388	DP1525	0.2
22	25-wc0.5p0.5				0.5
23	26-wc0.4p0.3	0.4	0.442	DP1526	0.3
24	26-wc0.5p0.3	0.5	0.388		
25	26-wc0.6p0.3	0.6	0.346		
26	26-wc0.5p0.2	0.5	0.388	DP1526	0.2
27	26-wc0.5p0.5				0.5
28	23-wc0.7p0.3	0.7	0.312	DP1523	0.3
29	24-wc0.7p0.3	0.7	0.312	DP1524	
30	25-wc0.7p0.3	0.7	0.312	DP1525	
31	26-wc0.7p0.3	0.7	0.312	DP1526	

Table 2: The characteristics of four types of lignosulfonate (LS)

Characteristic	DP1523	DP1524	DP1525	DP1526
DM, %	40	40	40	40
Mw	45700	35000	87100	6000
Mn	2650	2650	5100	1250
pH, 10% solution	7.8	4.4	8.2	6.8
Insoluble, w/w %	0.03	0.67	0.01	0.5
Reducing sugars, %	0.8	7.3	<0.5	4.1
Calcium, %	0.4	4.6	0.03	6.6
Sodium, %	8.8	0.4	6.1	0.2
Chloride, %	<0.05	<0.05	<0.05	0.2
Sulphate, %	1.5	0.4	0.5	0.2

Table 3: The characteristics of Portland cement

Composition	SiO_2	Al_2O_3	Fe_2O_3	CaO	MgO	P_2O_5	K_2O	Na_2O	SO_3	Blaine [m^2/kg]	D_{50} [µm]	Specific weight [g/cm^3]
STD-CEM I	20.98%	5.13%	5.13%	60.61%	2.39%	0.14%	0.86%	0.43%	3.01%	382	13.3	3.15

2.2. Measurement methods

The HYSPT setup is shown in Fig. 2 and also described elsewhere [7, 9]. The pressure sensors can be mounted at different depths, in this work the pressure variation was recorded at 1, 2, 4, 6, 11 and 20 cm depths by filling fresh cement paste to a proper height above the sensors. HYSPT is a gravimetric method that applies sensitive pressure sensors to detect low pressure changes mainly induced by the movement of particles and fluid [6, 7, 9]. The small drop in hydrostatic pressure during the first couple of hours of fresh cement paste before set is of a different nature than the formwork pressure reduction that normally is monitored over longer time. Using a model proposed by Ovarlez and Roussel [27] the formwork pressure at 10 cm height (approximately middle of the cylinder) at a filling rate of 0.1 m/s and a thixotropic structuration rate of 0.1 m/s is estimated to be around 100 Pa assuming the cement paste density to be 2000 kg/m^3. It is emphasized that much of the variation in the sedimentation rate takes places at heights above 10 cm where the contribution from formwork pressure will be smaller. As will be shown below, this is substantially less than the measured change in hydrostatic pressure due to sedimentation.

To the best of our knowledge, use of a change in hydrostatic pressure to detect cement particle movement was first published in 1976 [28, 29]. The estimated counter-flow due to chemical shrinkage at the setting point (around 3% degree of hydration [30]) leads to less than 10% of the pure hydrostatic pressure drop according to our estimates based on Darcy and using realistic permeability values for fresh paste [31, 32]. The left plot in Fig. 3, taken from Radocea [33] illustrates the pressure mechanisms in the different phases during settling and setting of fresh cement paste. HYSPT measurements were found to match this illustration [34], as shown in the right plot of Fig. 3. Note that the Endress & Hauser Cerabar S PMC71 pressure sensor used in HYSPT self-compensates the atmospheric pressure variations and thus records pure hydrostatic pressure change with an accuracy of 0.75 Pa. The sedimentation rate expressed as dP/dt from HYSPT takes into account the solid fraction variations in all zones above the detection level, while the much larger formwork pressure includes water suction by the water-air menisci formation between particles at the surface, thixotropic structural buildup and the more powerful suction due to chemical shrinkage after paste set. It should be noted

that the right plot in Fig. 3 does not include pressure variation due to evaporation since it is always avoided in HYSPT. The hydration for all conditions has been determined with isothermal calorimetry [34] to make certain that all samples are in the induction period [35] during sedimentation measurements. Earlier research on static yield stress buildup of such pastes [34] by plate test [36] has validated that the pressure induced by thixotropy and yield stress buildup in the early age (4 h in this case) is limited to less than about 10% of the pressure drop due to particle movement. Based on above discussion and Fig. 3, it can be inferred that pressure drop followed by a plateau pressure equal to water pressure at that level is presumably due to particle movement. This is further studied here by progressively moving the detection level closer to the liquid surface and using Turbiscan measurements.

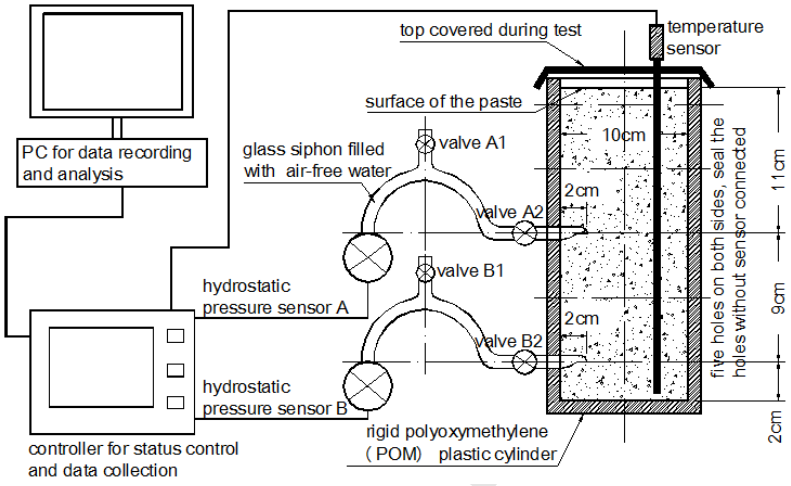

Fig. 2: hydrostatic pressure test pressure detection system (sensors at 11 and 20 cm depth)

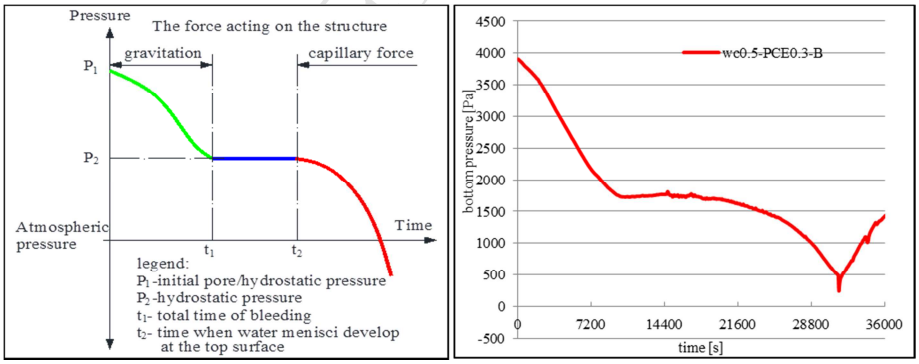

Fig. 3: Left – the pressure acting on paste structure illustrated by Radocea [19]; right – the pressure measured by HYSPT at the bottom level of the paste with w/c=0.5 and 0.3% PCE [34]

The visual bleeding test comprises a glass cylinder with 65 mm diameter filled to the same height of paste sample as the HYSPT column (22 cm). The cylinder was always covered with plastic foil to avoid evaporation. In Fig. 4 a typical result with the effect of LS is shown. It can be seen that the visual bleeding of paste with 0.3% LS is larger than that of paste with 0.5% LS. However, the paste with the high amount of LS has a deep soft turbid layer. This soft turbid layer is not detected by simple visual observation.

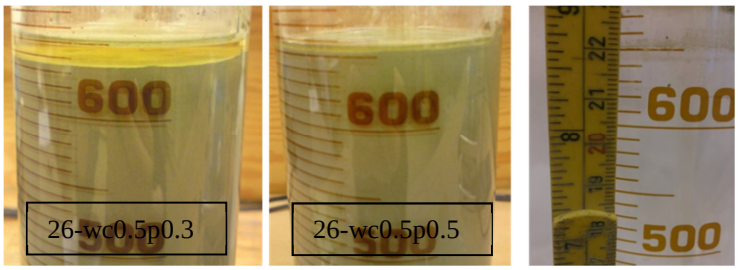

Fig. 4: Visual bleeding measurements for pastes at 4 h (right picture for reference to dimension)

The turbidity measurements were performed by using an optical Turbiscan analyzer [37]. It can record destabilization of concentrated dispersions with solid volume fraction up to 60% and mean particle sizes between 0.05 and 5 μm. The apparatus is programmed to scan along the height of the cement paste every minute for the first hour and every third minute for the other three hours, and acquires both the transmitted light (at 180° to incident light) and backscattered light (at 45° to the incident light). The stability of the paste can be evaluated by analyzing the variation in transmitted or backscattered intensity at different times. The paste is stable if the scans at different times overlap. It is assumed that a change in the transmission value ΔT corresponds to a change in the particle volume fraction due to particle migration or flocculation. An increase in transmission at a specific height is assumed to correspond to the incipient stages of bleeding layer formation. The evolution of the bleeding process is described by the increase in both height and transparency as a function of time with the software Turbisoft LabExpert V.1.13. An example of measured transmission as a function of height and time in the first 2 h for two pastes with different LS is presented in Fig. 5.

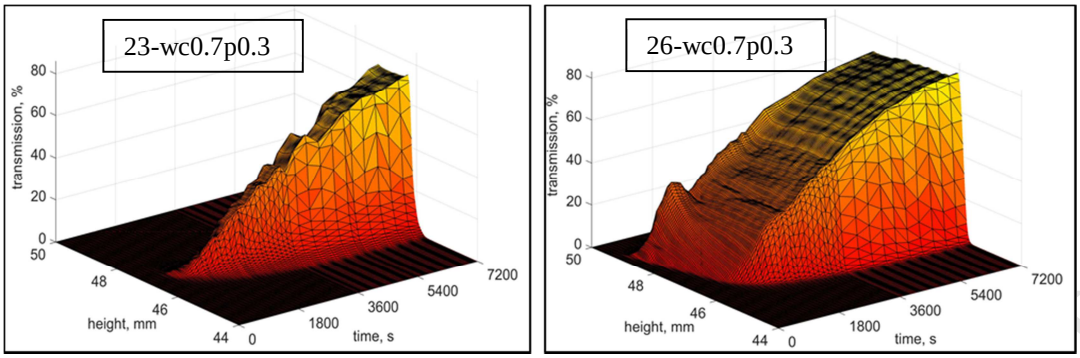

Fig. 5: A 3D illustration of bleeding formation based on the variation of transmission as a function of height and time

The pastes are completely turbid and no light penetrates at the onset of the experiments, characterized by zero transmission. For the right plot, after around 10 min a small shoulder appears near the top of the paste which widens to span the entire height of the bleeding layer after around 20 min. As time goes, the transparency of the bleeding layer increases corresponding to a gradual clarification. This variation provides an independent description of the sedimentation process since the transmitted light is inversely proportional to the volume fraction of particles. The results shown in Fig. 5 indicate that the formation of a bleeding layer is different in the presence of the two LS. For the paste containing 0.3% DP-1523 LS (left in Fig. 5), the transmitted light increases centered along a narrow band of heights; in contrast, sedimentation in the paste containing 0.3% DP-1526 (right in Fig. 5) takes place in a wider band of sample heights. With addition of DP-1523, the bleeding layer remains as a ≈ 1 mm narrow band for 4 h. In contrast, the bleeding layer of paste containing DP-1526 rapidly expands to around 3 mm. The transmitted light intensity gradually increases up to 80% in 2 h after which the intensity gradually increases in the last 2 h of tests for both pastes. The gradual transmission increase signifies the emergence of a bleeding layer. The software facilitates calculation of the band width where sedimentation takes place. The lower part of this band corresponds to the non-transparent part of the paste and the upper part equals to the surface of the paste. The formation of a soft turbid bleeding zone can be due to the presence of plasticizer. Fig. 5 illustrates the effects of different plasticizers on this process, while currently the reason for such effects cannot be explained. More details about Fig. 5 will be discussed in the section about Turbiscan results.

The data shown in Fig. 5 are used to calculate the bleeding height as a function of time. To get the bleeding height from the transmission light change ΔT, it is important to define a proper threshold of ΔT that can be looked on as the bleeding layer. A low transparency threshold of 0.3% was selected to capture the different sedimentation processes of various pastes. Selection of a higher transparency threshold value does not change the appearance of the calculated bleeding height. It does shift the onset of bleeding to longer times and lowers the bleeding height. 0.3% transparency threshold does not correspond to completely transparent water but reflects that the solid fraction at a given height is lower than the initial one. It means that the transparency change captures the bleeding formation. The bleeding heights as a function of time observed in Fig. 5 with such threshold definition are presented in Fig. 6. All bleeding results in the following sections are presented in the same way.

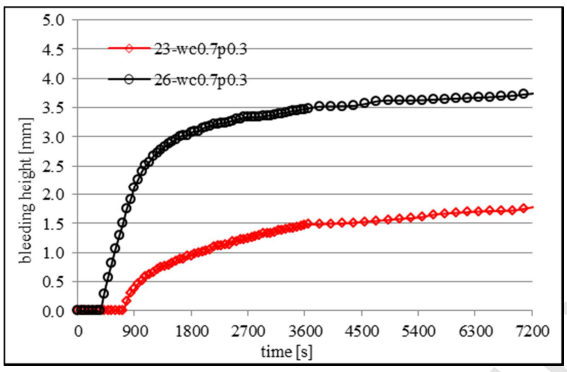

Fig. 6: The bleeding height measured Turbiscan (transmission light) for two pastes with different LS

Turbiscan monitors the bleeding process precisely by detecting the change in transmitted light. However, the vials used in Turbiscan measurements have smaller diameter than those for the other methods. Compared with the bigger containers in HYSPT and visual bleeding tests, the size of the Turbiscan vial may induce wall effects as the surface/volume ratio is higher than the other cylinders [34]. Green and Boger [38] found that a smaller container diameter restricts particle migration. At the beginning of Turbiscan experiment, a horizontal border forms at the top of sample. However, the bleeding water gradually wets the vial wall and forms a curved meniscus. As the meniscus represents an interface between the sample and the top phase, the instrument records the meniscus with different transmission than the sample or bleeding water. The meniscus curvature is determined by the air-water interfacial tension (which will be further increased due to the presence of ions released from the cement) and the wetting- or contact angle of the glass. The water below the meniscus is detected as

bleeding zone. If the meniscus curvature is high, the bleeding zone detection will be delayed until a "transparent" layer forms below the meniscus. In addition, the water captured in the meniscus cannot be detected. In order to lower the interfacial tension between bleeding water and the top phase, a thin layer of silicone oil containing a small amount of surfactant (water-soluble linear alcohol) was added on the top of the paste prior to Turbiscan measurements. The difference in meniscus curvature with air, only silicone oil or oil with surfactant is illustrated in Fig. 7.

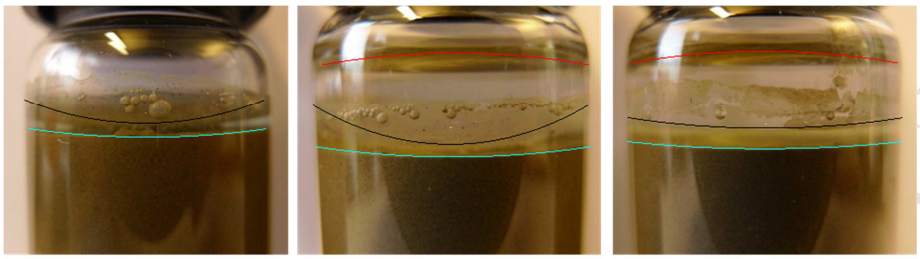

*note: blue line - top of sediment cake; black line - top of bleeding; red line - top of oil

Fig. 7: The menisci of normal paste (w/c=0.6) without oil top (left), with only oil top (middle) and with oil combined surfactant on top (right)

The repeatability of Turbiscan was investigated, see Fig. 8 for the pastes with w/c=0.6, wc0.6 for the cases without oil top and wc0.6-ot for that with oil and surfactant. Turbiscan measurements without oil top show good repeatability with lower than 1% variation of total bleeding in 4 h. In the case with oil top, the bleeding was observed around 20 min earlier than the case without oil top. We assume this corresponds to the time required for the meniscus to pass the detector. Finally the bleeding height from the oil top measurement is much higher. As discussed above, using oil with surfactant on top facilitates an earlier bleeding detection because the meniscus towards the oil has a lower curvature, which also results in a higher bleeding height. However, the features of the curves in Fig. 8, which present the bleeding rate, are similar which indicates that the measurements with or without oil top both show the bleeding layer buildup. More results for the measurements with or without oil top will be presented in the following section.

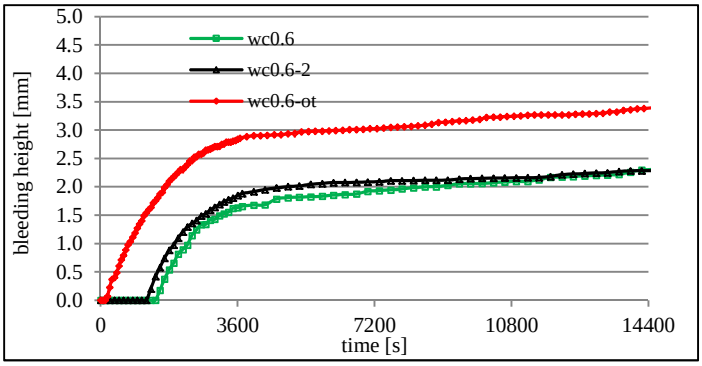

Fig. 8: bleeding heights of pastes with w/c=0.6 measured by Turbiscan with or without oil top in 4 h

3. Results and discussion

3.1. Clear bleeding measured by visual bleeding test

The total visual bleedings of all cement pastes in 4 h are shown in Fig. 9. The legend from top to bottom corresponds to the paste codes with their bleeding heights shown from left to right. It is reasonable that the bleeding height increases notably with increased w/c ratio. However, from the results of the paste groups with w/c=0.5, it is interesting that bleeding heights do not change with increasing LS dosage. The effects of different LS on clear bleeding depth vary with the w/c ratio and the dosage. Fig. 9 also shows that for group w/c = 0.5, the paste with 0.3% DP1523 presents slightly higher bleeding than those with 0.2% or 0.5% dosages. DP1524 induces lower bleeding as dosage increases from 0.2% to 0.5%, whereas DP1525 and DP1526 do not present any clear tendency. This means that different types and amounts of LS may change the flocculation state of the paste which is observed as changes in the bleeding height. The visual observation of bleeding neglects the possible turbid bleeding layer, which is a weakness. It may explain why these results are not in line with the sedimentation process shown in Fig. 10 to 12 further on below.

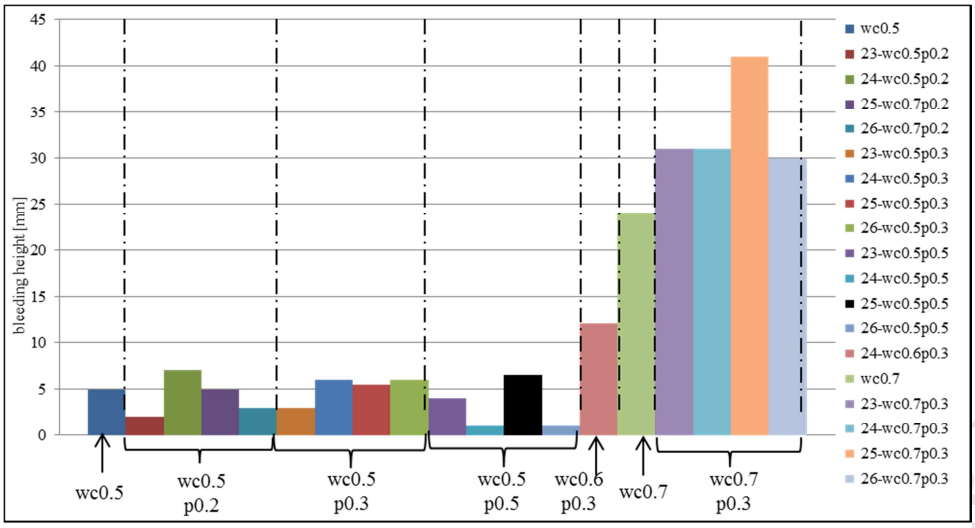

Fig. 9: the visual bleeding heights of cement pastes after 4 h sedimentation

3.2. Sedimentation process measured by HYSPT

The changes in hydrostatic pressure as a function of time for cement pastes with different LSs are shown in Fig. 10 to 12. The left parts of all figures show the bottom pressure at 20 cm below the paste surface and the right for the middle pressure at 11 cm below the surface. A plateau pressure is reached in 4 h for some measurements. This constant pressure is similar to the water pressure above the sensor which again validates the previous inference about particle movement. Attainment of theoretical hydrostatic pressure of water signifies that the particles above the sensor are part of a percolated network supported by the bottom of the container. In contrast, a decaying hydrostatic pressure, larger than that of water, signifies that particles are still suspended and sinking above the pressure sensor. Earlier in [7] it was assumed that the paste close to the pressure sensor at the middle level belongs to the homogeneous zone (Fig. 1). The pressure sensor at the bottom was assumed to record the pressure variation in the sediment cake. Using these assumptions and Eq. (2) allow calculation of the bleeding height as a function of time. Fig. 10 shows the pressure variations for cement pastes with w/c=0.5 and 0.3% of different LS, and Fig. 11 corresponds to the effects of 0.5% LS. Generally the sedimentation process at the measurement point ends when the plateau of water pressure is reached. The presence of LS influences this process in two ways: firstly the plateau establishes with a less clear nick point, secondly the time to reach the equilibrium pressure and the whole sedimentation period can be

prolonged. Possible causes are general dispersion of the cement particles and modulated interparticle forces which may facilitate higher packing densities in the variable concentration zone and sediment cake. However, the influences vary with the type and dosage of LS. The different LSs dosed at 0.3% lead to rather similar pressure reductions with time. Fig. 11 shows a slower decay of pressure in the presence of DP-1525 than the other LSs. This may pertain to the higher molecular weight of DP-1525 which stabilizes the paste better than the other LSs. Earlier research by Wallevik [39] also showed that high molecular weight LS at higher dosage, 0.6% in his case, induces higher plastic viscosity of the fluid phase of paste or mortar phase which reduces the particle sinking velocity according to Stokes Law [10]. However, at lower dosage such as 0.3% this effect is not obvious. Possibly there is a critical dosage of LS for cement paste depending on the solid fraction (or w/c ratio) where all the particles are dispersed well but without more LS left in the fluid. In addition, the previous research with HYSPT [7] showed the pastes without plasticizer (sample 1-4) presented a relative higher pressure drop gradients and sedimentation rate compared with the pastes with the same w/c ratio and SP. The dispersing effect of SP and thus less flocculation mainly contributes to this effect according to Stokes' Law [10].

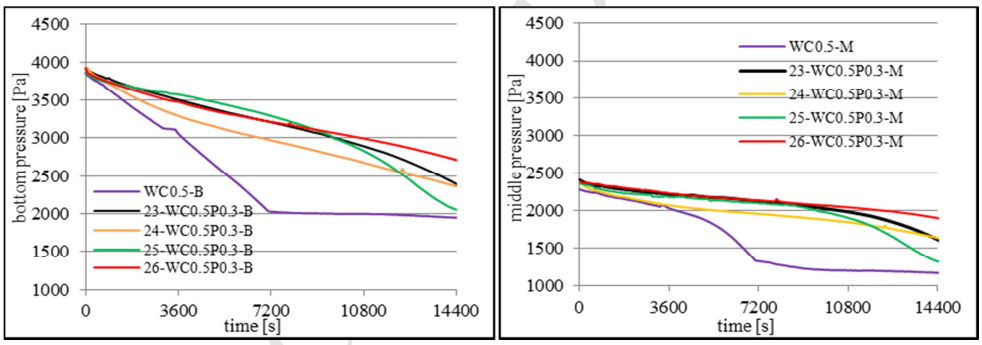

Fig. 10: The pressure results of cement pastes with 0.3% of different LS

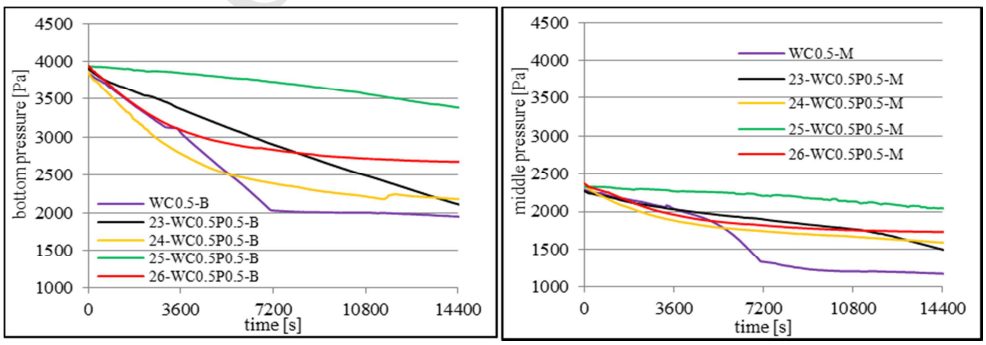

Fig. 11: The pressure results of cement pastes with 0.5% of different types of LS

The sedimentation processes for cement pastes with the same LS and various w/c ratios are shown in Fig. 12. The variations in initial pressure are mainly the consequence of different initial densities and a small variation in filling height of the samples. The pressure drop with time for w/c=0.4 is more rapid than for w/c 0.5 and 0.6. It may happen for three reasons. First, more extensive flocculation happens due to the shorter inter-particle distance and the enhanced attractive forces between particles. Secondly the sediment cake and variable concentration zones occupy larger fractions of the paste with lower w/c ratio which may change the hydrodynamics of the sedimentation process. Finally the lower w/c ratio also causes more autogeneous shrinkage and higher rate of chemical shrinkage [40, 41] as a result of the earlier reactions between cement and water, which lead to the volume reduction.

Fig. 10 to 12 illustrate that the pressure change can be divided into two phases: an initial fast pressure drop period followed by a plateau period with diminishing rate. It matches the two bleeding phases presented in the introduction. The period before reaching the plateau can be defined as the bleeding period. Radocea [33] claimed that after this period menisci form at the surface causing suction where evaporation took place. He called this the setting of cement paste, see also Fig. 3. In this research the surfaces of all pastes are wet without menisci formed between particles. Evaporation is eliminated by the foil on the cylinder top but the re-suction by chemical shrinkage persists. Two additional findings can be pointed out. First, the pressure does not decrease at a constant rate for some pastes with LS. It reflects various bleeding rates with time. Secondly, the pressure curves at bottom and middle levels for a specific paste do not always show the same shape because they might be within different sedimentation zones (see Fig. 1 and 2).

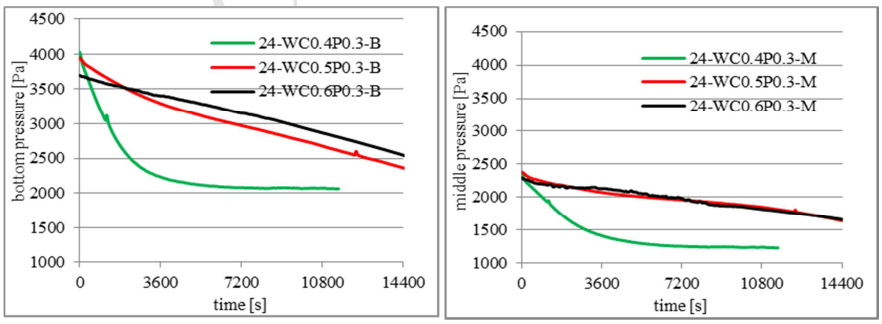

Fig. 12: The pressure results of cement pastes with varied w/c ratios

3.3. Bleeding by near-surface pressure measurements with HYSPT

According to Eq. (2), bleeding can be properly calculated if the variation in solid fractions during the course of the sedimentation process above the pressure detection level is known. It was found in [9] that the homogeneous zone below the turbid bleeding zone has a solid volume fraction close to the initial solid fraction of the paste. When just measuring the pressure below the surface, potentially only the bleeding and homogeneous zones are involved in the pressure changes. Therefore the bleeding rates as a function of time can be investigated by HYSPT with the pressure transducers installed close below the bleeding front applying Eq. (2). Fig. 13 shows the top pressure changes at 2 cm below the top surface for the pastes with w/c = 0.7 and different LSs at 0.3% dosage. It can be seen that LS addition at this dosage influence on the particle sedimentation process by prolonged time to reach the plateau and plateau pressure closer to that of pure water ($p=\rho gh=1000\ kg\cdot m^{-3}\cdot 9.81\ kg\cdot m\cdot s^{-2}\cdot 0.02\ m\approx 200$ Pa). In addition, it is important to note the different natures of the plateaus at the middle or bottom level where the particles above the sensor are supported by the bottom of the container through a continuous percolated network (Fig. 10, 11 and 12), and at the top level where all particles have passed the sensor (Fig. 13).

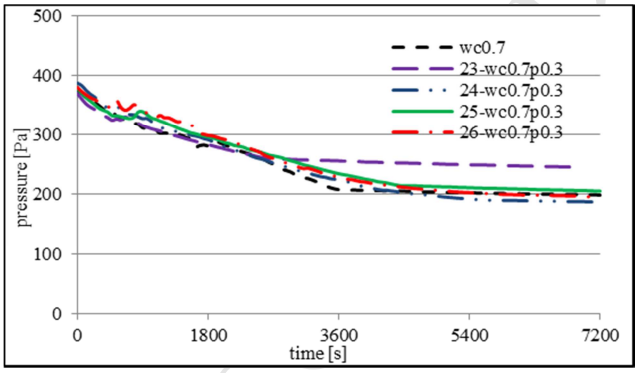

Fig. 13: Pressure measured at 2 cm below the paste surface for pastes with different LSs

Fig. 14 presents the calculated bleeding height and average bleeding rates in each 10 min for the first 2 h as a function of time based on Fig. 13 and Eq. (2) for the pastes with w/c=0.7. The bleeding rate at zero time cannot be calculated based on the equation and thus was not included in the bleeding rate curves (same for all other plots of bleeding rates). Generally the bleeding rates vary between $6.7\cdot10^{-06}$ and $7.6\cdot10^{-06}$ m/s in the first hour which are higher but in the same order of magnitude as determined from visual bleeding measurements ($2.1\cdot10^{-06}$ to $2.9\cdot10^{-06}$ m/s). K-C Eq. (Eq. (1)) gives a bleeding rate

of $2.2 \cdot 10^{-06}$ m/s, hence close to those from visual bleeding tests. The similarity between visual bleeding and the estimate from the K-C equation is reasonable since neither take the soft turbid layer into account. In contrast, HYSPT predicts larger bleeding rate when using Eq. (2) because the soft turbid layer has a lower density than the paste below it. After around 1.5 h, all the bleeding curves reach a plateau corresponding to the start of the second bleeding period with diminishing rate. Fig. 15 shows the bleeding heights and rates of paste with various w/c ratios. The pastes with w/c=0.5 and 0.6 show similar bleeding inflection points and rates but much lower than that with w/c=0.7, which is in line with visual bleeding tests. In addition, another interesting phenomenon observed by HYSPT is: the peaks of bleeding rates for all pastes occur during the first half hour, which matches with the observation by Turbiscan and will be explained later.

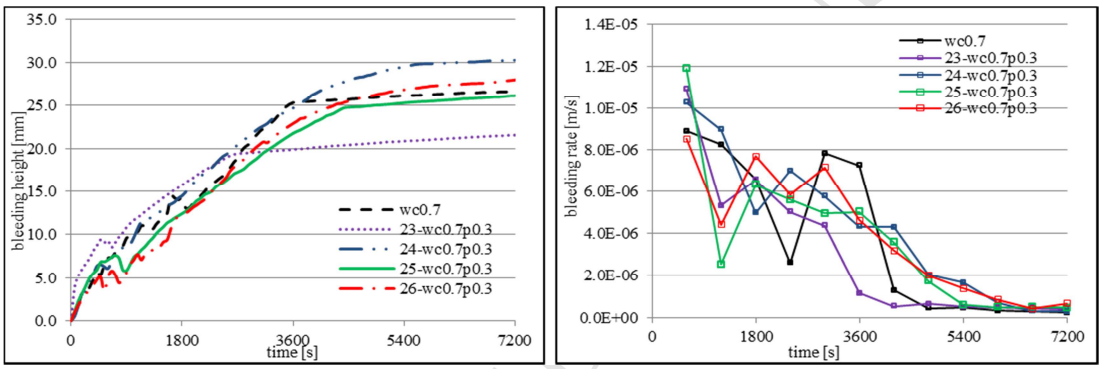

Fig. 14: Bleeding heights and bleeding rates calculated from HYSPT at 2 cm below surfaces for pastes with w/c = 0.7

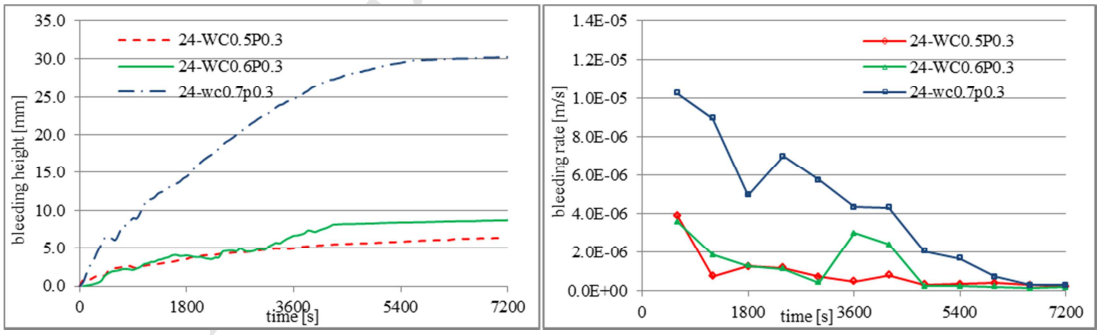

Fig. 15: Bleeding heights and bleeding rates for pastes with various w/c ratio

When the bleeding front is below the tip of the pressure sensor, the pressure reaches a plateau and bleeding cannot be observed as change in hydrostatic pressure. Therefore, the pressure sensor needs to be set close below the final bleeding front to observe the whole bleeding process. Fig. 16 shows the bleeding heights and rates calculated from the pressure variation at 2, 4 or 6 cm below the surfaces of

the pastes with w/c=0.7 and 0.3% LSs. The bleeding rates from the pressure variation at 4 and 6 cm are similar at $5 \cdot 10^{-06}$ m/s while the rate at 2 cm is higher at $7 \cdot 10^{-06}$ m/s. Only the bleeding curve at 2 cm reaches a plateau indicating that the bleeding front passes and finally forms at a lower height. Generally the bleeding rate seems fairly constant during the first hour which is in line with classic bleeding theory [1].

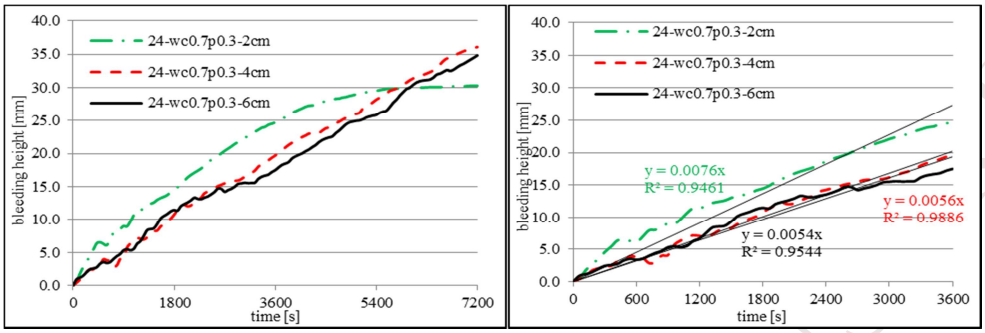

Fig. 16: Bleeding heights calculated from HYSPT at different levels (left-2 h, right-1 h with trendlines)

3.4. Clear and turbid bleeding measured by Turbiscan

3.4.1. Evolution from turbid to transparent bleeding observed by Turbiscan

Turbiscan was applied to observe the bleeding and sedimentation development first without adding oil layer on the top of the samples. The evolution of bleeding is shown in Fig. 17 for pastes with w/c = 0.7 and 0.3% LSs. The right plot shows the change of average bleeding rate calculated in steps of 10 min for the first 2 h from the left Turbiscan results. From the start, zero bleeding height indicates that the paste is turbid and no light can travel through. At different times depending on the type of LS, a bleeding layer starts to form with two processes: one fast initial followed by a slower. Both rates vary with the type of LS. After around 1 h, the bleeding height attains a steady lower value. The final bleeding layers also have different heights after 2 h compared to after 1 h. The bleeding rates from Turbiscan measurements shown in Fig. 17 seem lower than those from HYSPT possibly due to the size effects mentioned in Section 2.2. The pastes with various LS show different maximum bleeding rates which occur at the same time. A common feature of the bleeding rates is a quick acceleration to a peak bleeding rate from an apparent zero rate and then a somewhat slower decay towards zero again.

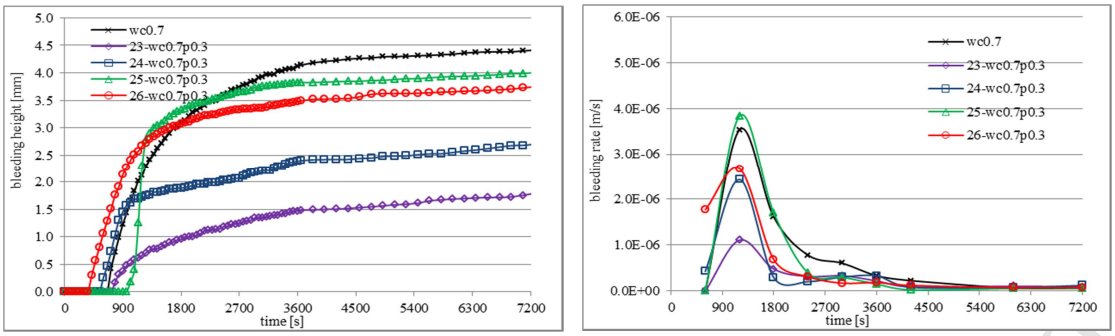

Fig. 17: Calculated evolution of bleeding height and bleeding rate for pastes with various LS

Going back to Fig. 5, one may discern that the initial thin bleeding layer maintains high light transmission during the whole experiment. During early sedimentation the bleeding gradually increases to a maximum depth and then remains constant afterwards until the experiments ends. Fig. 5 indicates that the height of bleeding layer is established within the first 20 min and becomes more transparent over the course of several hours. Possibly the fast bleeding process corresponds to the fast sedimentation of the top particles and the formation of turbid bleeding layer at a relative constant rate. When the bulk of particles have passed through the bleeding front, it corresponds to a lower bleeding rate and a gradual clarification of the bleeding layer seen as an increase in the transmission, see Fig. 5 after around 1 h. The Turbiscan observations indicate that the formation of the bleeding zone in Fig. 1 can be described as the following two stage process. First a short-term hindered sedimentation of particles and fluid flowing upwards to form the main bleeding layer, then follows a long-term supernatant clarification and sediment compression. The latter is characterized by high and increasing degree of particle percolation that transfers load from the solids to the bottom of the container by direct contact, hence reducing hydrostatic pressure to water pressure.

3.4.2. Materials effect on bleeding by Turbiscan with oil top setup

Fig. 18 shows bleeding of plain pastes with various w/c ratios observed by Turbiscan with oil top. It can be seen that the time to establish the bleeding layer increases with the initial solid fraction of the paste. It is interesting that the bleeding height continues to increase during the whole measurement period for the pastes with w/c=0.6 and 0.7, while it decreases for pastes with w/c =0.4 and 0.5 after around 1 h. Probably the bleeding height decreases due to the stronger chemical shrinkage and water

re-suction for pastes with lower w/c ratio. Furthermore it seems that LS has two effects on bleeding: first the water re-suction is relieved due to the retardation of cement hydration by LS; secondly the onset of bleeding is delayed, as also shown in Fig. 19 to 21. This is because LS disperses cement and these better dispersed particles sink more slowly delaying clarification.

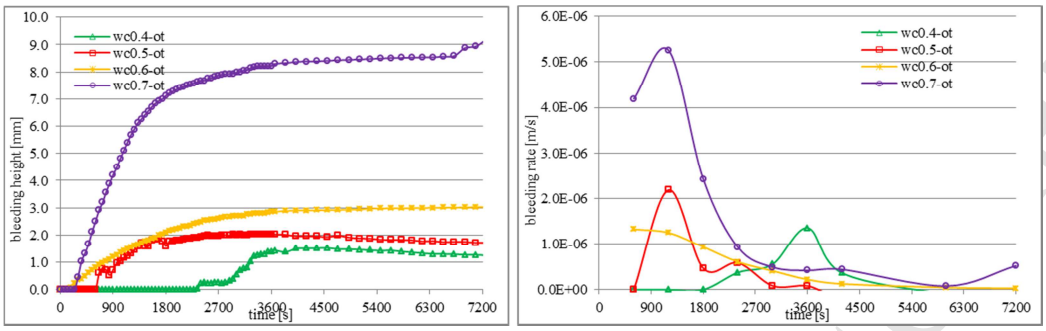

Fig. 18: Bleeding heights and rates for pastes with different w/c ratios

The effect of different LS on bleeding is compared in Fig. 19. The onset of bleeding layer follows the order DP1526<DP1523<DP1524 while the height of the final bleeding height presents the opposite order. As explained in [9], the plasticizer may improve dispersion of the cement particles and modify compression of the sediment cake, both modifying the stability of the cement paste. More effective LS affect both the onset of bleeding and bleeding height by reducing the particle settling rate and increasing the distance between particles, thus making the paste more stable. However, the paste with lower bleeding height observed by Turbiscan (Fig. 19) presents higher sedimentation rate shown in HYSPT (Fig. 10). This may reflect different measurement principles: the gravimetric HYSPT takes sedimentation of all particles above the detecting level into account, while the transmission light of Turbiscan only detects movement in the very thin bleeding layer at the top.

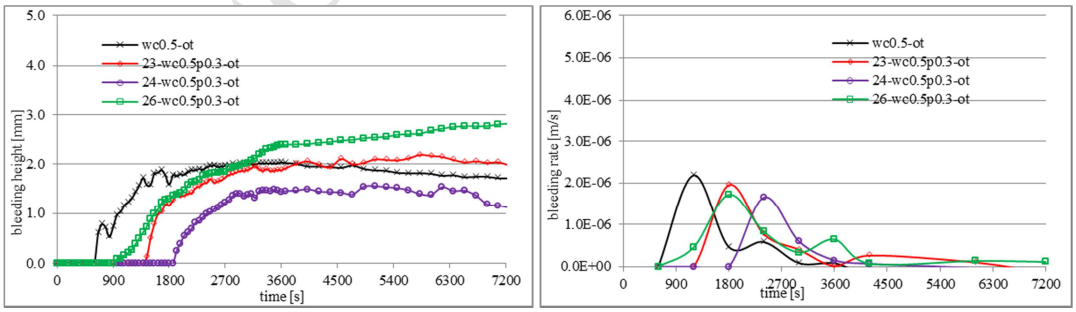

Fig. 19: Bleeding height and rate by Turbiscan measurements for pastes with w/c=0.5 and different LS

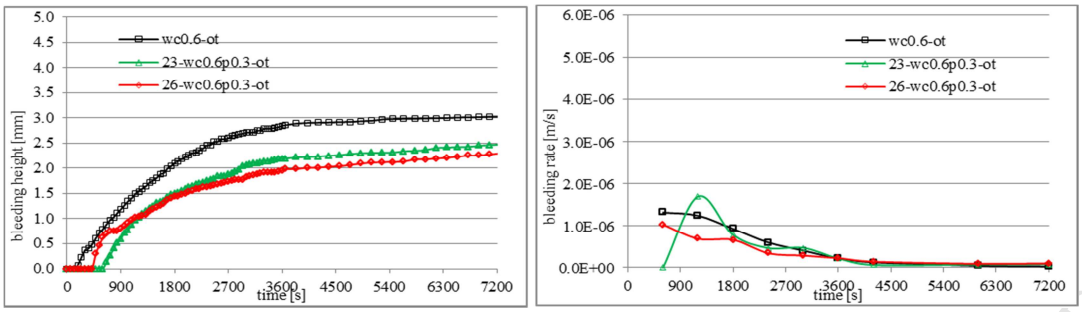

Fig. 20: Bleeding height and rate by Turbiscan measurements for pastes with w/c=0.6 and different LS

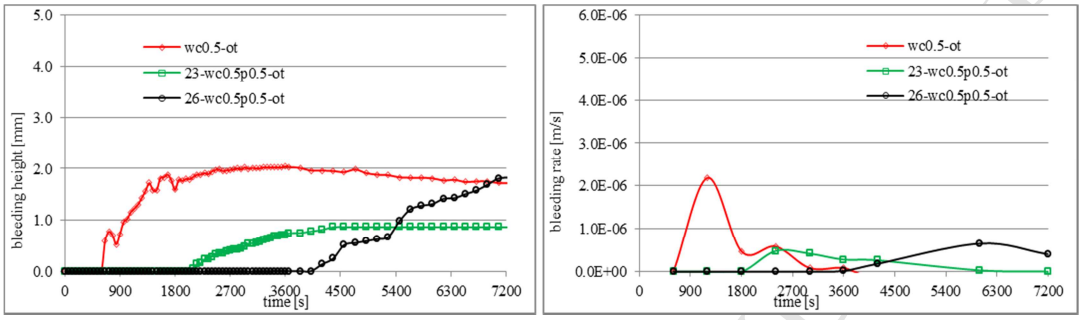

Fig. 21: Bleeding heights and rates by Turbiscan measurements for pastes with w/c=0.5 and different LS at the dosage of 0.5%

Fig. 20 shows the effect of DP1523 and DP1526 at higher w/c ratio. Comparing with Fig. 19, it is clear that LS acts as a better stabilizer against bleeding for pastes with lower w/c. On the other hand, Fig. 21 shows the dosage effect of different LSs (DP1523 or DP1526). Comparing Fig. 19 and Fig. 21, it seems that at w/c=0.5, higher dosage of LS delays the onset of bleeding and reduces the total bleeding. The paste with DP1526 presents a higher bleeding height after 2 h than that with DP1523, possibly resulting from the higher molecular weight of DP1523 and a better stabilizing effect. However, this effect is less clear for the paste with higher w/c ratio such as 0.6, as shown in Fig. 20.

3.5. Comparing bleeding rates by Turbiscan, visual bleeding, HYSPT and K-C Equation

The time that separates the two stages of the bleeding process (1 initial fast and 2 diminishing) are assumed to be the inflection points on the curves in Fig. 18-21. HYSPT results in Fig. 10-12 and Fig. 14-15 also show nick points but they cannot represent the start of diminishing bleeding period because the detected pressure may involve the fractional change of not only the bleeding but also all zones above the detecting level.

Table 4: all calculated bleeding in fast bleeding period and the first 2 h with parallel measurement results and K-C Eq.

cement paste code	Test method 1: visual bleeding	fast initial bleeding period 1 defined by Turbiscan	Test method 2: Turbiscan			Test method 3: HYSPT			calculated bleeding rate by K-C Eq. (Eq. 1)
	average bleeding rate in 2 h		aver. dh/dt in fast initial period 1 (< nick point)	average dh/dt in dismishing period 2 (nick to 2 h)	Notes	average dh/dt in period 1	average dh/dt in period 2	Notes	
	[m/s]		[m/s]	[m/s]		[m/s]	[m/s]		[m/s]
wc0.7	$1.9\cdot 10^{-5}$	0.5	$2.0\cdot 10^{-6}$	$3.0\cdot 10^{-7}$	calculate from Turbiscan without oil top setup	$7.9\cdot 10^{-6}$	$2.3\cdot 10^{-6}$	calculate from top pressure	$4.8\cdot 10^{-6}$
23-wc0.7p0.3	$2.6\cdot 10^{-5}$	0.5	$6.4\cdot 10^{-7}$	$1.8\cdot 10^{-7}$		$7.8\cdot 10^{-6}$	$1.4\cdot 10^{-6}$		
24-wc0.7p0.3	$2.6\cdot 10^{-5}$	0.5	$1.3\cdot 10^{-6}$	$1.8\cdot 10^{-7}$		$8.1\cdot 10^{-6}$	$2.9\cdot 10^{-6}$		
25-wc0.7p0.3	$3.3\cdot 10^{-5}$	0.5	$2.2\cdot 10^{-6}$	$1.5\cdot 10^{-7}$		$6.9\cdot 10^{-6}$	$2.5\cdot 10^{-6}$		
26-wc0.7p0.3	$2.5\cdot 10^{-5}$	0.5	$2.2\cdot 10^{-6}$	$1.5\cdot 10^{-7}$		$6.9\cdot 10^{-6}$	$2.9\cdot 10^{-6}$		
wc0.4	/	0.5	$4.5\cdot 10^{-7}$	$1.6\cdot 10^{-9}$	calculate from Turbiscan with oil top setup	/	/	calculate from middle pressure	$1.4\cdot 10^{-6}$
wc0.5	$4.5\cdot 10^{-6}$	1.0	$6.8\cdot 10^{-7}$	$1.1\cdot 10^{-7}$		$9.0\cdot 10^{-6}$	$5.4\cdot 10^{-6}$		$2.1\cdot 10^{-6}$
wc0.6	/	1.0	$9.3\cdot 10^{-7}$	$7.0\cdot 10^{-8}$		/	/		$2.9\cdot 10^{-6}$
wc0.7	$1.9\cdot 10^{-5}$	0.5	$4.8\cdot 10^{-6}$	$3.6\cdot 10^{-7}$		/	/		$3.8\cdot 10^{-6}$
24-wc0.4p0.3	$1.4\cdot 10^{-6}$	1.0	$9.5\cdot 10^{-7}$	$7.0\cdot 10^{-7}$		$4.8\cdot 10^{-6}$	$2.9\cdot 10^{-6}$		$1.4\cdot 10^{-6}$
24-wc0.4p0.5		/	/	/		/	$3.5\cdot 10^{-5}$		/
wc0.5	$4.5\cdot 10^{-6}$	1.0	$6.8\cdot 10^{-7}$	$1.1\cdot 10^{-7}$		$9.0\cdot 10^{-6}$	$5.4\cdot 10^{-6}$		$2.1\cdot 10^{-6}$
23-wc0.5p0.3	$2.5\cdot 10^{-6}$	1.0	$6.1\cdot 10^{-7}$	$8.2\cdot 10^{-8}$		$6.5\cdot 10^{-6}$	$3.2\cdot 10^{-6}$		$2.1\cdot 10^{-6}$
24-wc0.5p0.3	$4.3\cdot 10^{-6}$	1.0	$4.8\cdot 10^{-7}$	$9.3\cdot 10^{-8}$		$8.0\cdot 10^{-6}$	$3.9\cdot 10^{-6}$		$2.1\cdot 10^{-6}$
25-wc0.5p0.3	$5.6\cdot 10^{-6}$	/	/	/		$6.4\cdot 10^{-6}$	$2.7\cdot 10^{-6}$		$2.1\cdot 10^{-6}$
26-wc0.5p0.3	$5.8\cdot 10^{-6}$	1.0	$8.0\cdot 10^{-7}$	$1.4\cdot 10^{-7}$		$5.3\cdot 10^{-6}$	$3.2\cdot 10^{-6}$		$2.1\cdot 10^{-6}$
23-wc0.5p0.5	$4.8\cdot 10^{-6}$	0.5	$0.0\cdot 10^{-7}$	$2.1\cdot 10^{-7}$		$7.1\cdot 10^{-7}$	$4.0\cdot 10^{-7}$		$2.1\cdot 10^{-6}$
24-wc0.5p0.5	$1.1\cdot 10^{-7}$	/	/	/		/	$1.0\cdot 10^{-5}$		$2.1\cdot 10^{-6}$
25-wc0.5p0.5	$7.2\cdot 10^{-6}$	/	/	/		/	$2.2\cdot 10^{-6}$		$2.1\cdot 10^{-6}$
26-wc0.5p0.5	$1.1\cdot 10^{-7}$	1.0	$7.3\cdot 10^{-8}$	$5.9\cdot 10^{-8}$		$9.0\cdot 10^{-7}$	$3.3\cdot 10^{-7}$		$2.1\cdot 10^{-6}$
23-wc0.6p0.3	/	1.0	$7.3\cdot 10^{-7}$	$9.3\cdot 10^{-8}$		/	/		$2.9\cdot 10^{-6}$
24-wc0.6p0.3	$1.3\cdot 10^{-5}$	/	/	/		/	$6.0\cdot 10^{-6}$		$2.9\cdot 10^{-6}$
26-wc0.6p0.3	/	1.0	$6.4\cdot 10^{-7}$	$1.2\cdot 10^{-7}$		/	/		$2.9\cdot 10^{-6}$

Table 4 shows the average bleeding rates in both fast and diminishing periods observed by three parallel methods and theoretical bleeding rates for all pastes. The average bleeding rate in the fast initial phase (left) and diminishing phase (right) for cement pastes with w/c=0.5 based on Table 4 is also presented in Fig. 22 for more intuitive comparison between different suspensions. The results in Table 4 show that most bleeding rates from Turbiscan with oil top, HYSPT and visual bleeding measurements are of the same magnitude for the fast initial bleeding phase but vary more for the diminishing period. The Turbiscan bleeding rates are obviously smaller than those of calculated rates based on HYSPT results and Eq. (2), probably due to the much smaller volume of samples and different measurement principles as discussed earlier. In addition, Eq. (2) might be too simplified when the middle pressure is applied to calculate bleeding rate because the solid volume fraction between bleeding front and the middle pressure detecting level varies too much. The top pressure measured by HYSPT close below the bleeding front seems better suited for evaluating bleeding rate. Though the average value could be close to experimental results, the theoretically constant bleeding rates calculated by the K-C Equation obviously cannot reflect the time-dependent bleeding rates which

are highly affected by sedimentation, compression, flocculation and particle dispersing phenomena etc. Similarly, bleeding rates from visual bleeding tests, which only take clear bleeding into account, only give average values similar to the K-C Eq.. The visual bleeding in a shorter period is hard to observe precisely, especially during the diminishing period with very slow increase of bleeding height for pastes with normal w/c ratios of approximately 0.5.

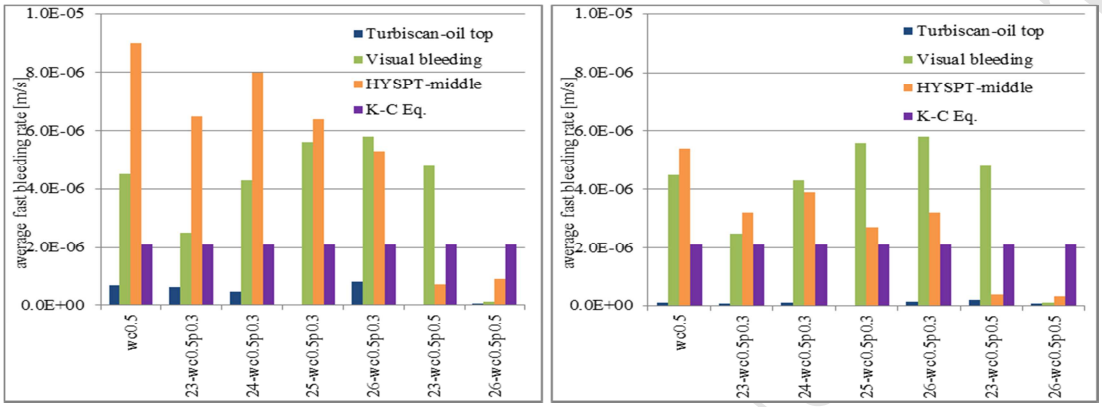

Fig. 22: Average bleeding rates in fast initial phase (left) and diminishing phase (right)

In Fig. 22, the bleeding rates in the fast initial period demonstrate how LS affect formation of the bleeding zone and lowers particle settling rate. The average bleeding rate in the diminishing period may reveal if LS affects compression of the sediment cake. Comparing bleeding rates from HYSPT in the two periods show that all LSs reduce bleeding rates in both periods. Various LSs induce different effects in the two periods. Finally it should be mentioned that in [34, 42] an early flash-setting behavior was observed for a few cement pastes with very high dosage of plasticizer, 0.8% LS for example. This affects HYSPT measurements by altering some fresh properties such as thixotropy and the complete loss of flow properties so that HYSPT is not applicable at such situation.

4. Conclusion

The mechanisms of bleeding in fresh cement paste were studied with two new measurement methods and the lignosulfonate effect on bleeding was investigated. The bleeding rate of fresh cement paste cannot always be regarded as constant as assumed by the Kozeny-Carman Equation (K-C, Eq. (1)) and in traditional bleeding measurements. A soft, or turbid, bleeding front can make visual observation unable to detect bleeding precisely. Two new measurement methods, HYdroStatic Pressure Test and

Turbiscan, were therefore applied for turbid bleeding observation. Traditional visual bleeding tests and K-C Eq. were compared with the former methods. Two bleeding stages (fast initial and diminishing) were observed by HYSPT and Turbiscan measurements with fluctuating rates. Turbiscan can define the movement of the bleeding front based on a selected threshold for the transmission light used to scan a paste sample which most clearly shows the two-phases bleeding. Adding a layer of thin oil and surfactant top on paste helped Turbiscan to get a clearer bleeding surface without artifacts by meniscii, thus achieving better bleeding results. HYSPT can be used to investigate bleeding and sedimentation because the detected pressure indicates the density change and thus solid volume fraction change due to particle movement and fluid flow above the sensor, and/or bottom support from the container by particle percolation below the sensor. For bleeding it is important to set the pressure sensor close below the bleeding front instead of too low or above it during the whole bleeding process. The calculated bleeding rates from HYSPT, Turbiscan and traditional visual bleeding tests had similar magnitude in the fast bleeding phase but were more different in the diminishing period. Generally visual bleeding tests and Turbiscan measurements were affected by the clarity of the bleeding zone. LS generally prolonged the sedimentation process and induced lower bleeding rates according to all experimental results. However, the four types of LS presented different influences due to types, dosages of LS and the various w/c ratios of cement pastes so that further research is needed to explain the various effects between the different LS.

Acknowledgement

The authors gratefully acknowledge the financial support by COIN (COncrete INnovation Centre), Department of Structural Engineering at NTNU and Borregaard LignoTech to this research.

References

[1] Powers T.C., “The Bleeding of Portland Cement Paste, Mortar, and Concrete”, ACI Materials Journal, V.35, 1939, pp.465-480, DOI: 10.14359/8504

[2] Darcy H., “Les Fontaines Publiques de la Ville de Dijon”, Victor Dalmont, Paris, 1856

[3] Sutera S. P., “The history of Poiseuille’s Law”, Fluid Mechanics, V.25, 1993, pp.1-19

[4] Carman P.C., “Fluid flow through granular beds”. MIT Chem Eng., V.15, 1937, pp.150-166.

[5] Powers, T. “The Properties of Fresh Concrete”, Wiley & Sons, London, 1968, 664 pp.

[6] Peng Y.; Jacobsen S., Weerdt K. D.; Pedersen B.; Marstrander B. B., “Overview of rheology parameters affecting stability of SCC”, proceedings: Tenth International Conference on Superplasticizers and Other Chemical Admixtures in Concrete, Prague, SP 288, 2012, pp.481-496

[7] Peng Y.; Jacobsen S., “Influence of water cement ratio, admixtures and filler on sedimentation and bleeding of cement paste”, Cem. Concr. Res., V.54, 2013, pp.133-142

[8] Daczko J.A., “Self-Consolidating Concrete: Applying What We Know”, CRC Press, 2012, 304p

[9] Peng Y.; Jacobsen S., Weerdt K. De; Pedersen B., “Model and methods for stability of fresh cement pastes”, ASTM-Advances in Civil Engineering Materials, Vol.3, 2013, pp.1–24, doi:10.1520 /ACEM20130097. ISSN 2165-3984

[10] Stokes G.G., Mathematical And Physical Papers, 1901, V.3

[11] Mohr B.J., Hood K.L., “Influence of bleed water reabsorption on cement paste autogenous deformation”, Cem. Concr. Res., V.40, 2010, pp.220-225

[12] Bjøntegaard Ø., Hammer T.A., Sellevold E.J., “On the measurement of free deformation of early age paste and concrete”, Cem Concr. Comp., V.26, 2004, pp.427-435

[13] Richardson J. F., Zaki W. N., “The sedimentation of a suspension of uniform spheres under conditions of viscous flows”, Chemical Engineering Science, V.3, 1954, p.65-73

[14] Rhodes M., “Introduction to particle technology”, 2008, John Wiley &Sons, Ltd, UK, ISBN 978-0-470-01428-8, 450p.

[15] Kynch G. J., “A theory of sedimentation”, Trans. Faraday Society, V.48, 1952, pp.166-176, doi:10.1039/TF9524800166

[16] Fitch B., “Kynch theory and compression zones”, AIChE Journal, V.29, 1983, pp.940-947

[17] Josserand L., de Larrard F., “A method for concrete bleeding measurement”, Mat. Struc., V. 37, 2004, pp. 666-670

[18] Sawaide M., Iketani J., “Rheological analysis of the behavior of bleeding water from freshly cast mortar and concrete”, ACI Materials Journal, V.89, 1992, pp.323-327

[19] Kaplan D., "Pompage des betons (concrete pumping)", research report of LCPC, OA36, 2001, 228p. [in French]

[20] Perrot A., Lecompte T., Khelifi H., Brumaud C., Hot J., Roussel N., "Yield stress and bleeding of fresh cement pastes", Cem. Concr. Res., V.42, 2012, pp.937-944

[21] Radocea A., "A new nethod for studying bleeding of cement paste", Cem. Concr. Res., V.22, 1992, pp.855-868

[22] Meunier G., "Le TURBISCAN: un nouvel instrument de mesure de phénomènes de démixtion dans les émulsions et les suspensions", Spectra Analyse, V.179, 1994, pp.53-58

[23] Meunier G., Mengual O., "A new concept in stability analysis of concentrated colloidal dispersions", 4th World Surfactants Congress CESIO, v.4, 1996, pp.301-313

[24] Mengual O., Meunier G., Cayré I., Puech K., Snabre P., "TURBISCAN MA 2000: multiple light scattering measurement for concentrated emulsion and suspension instability analysis", Talanta, V.50, 1999, pp.445-456

[25] Lemarchand C., Couvreur P., Vauthier C., Costantini D., Gref R., "Study of emulsion stabilization by graft copolymers using the optical analyzer Turbiscan", International Journal of Pharmaceutics, V.254, 2003, pp.77-82

[26] Autier C., Azéma N., Boustingorry P., "Using settling behavior to study mesostructural organization of cement pastes and superplasticizer efficiency", Colloids and Surfaces A: Physicochemical and Engineering Aspects, V.450, 2014, pp.36-45

[27] Ovarlez G., Roussel N., "A physical model for the prediction of lateral stress exerted by self-compacting concrete on formwork", Mater. Struct. V.39, 2006, pp. 269-279

[28] Roffle J.F., "Pressure variation within concentrated settling suspensions", J. Phys. D: App. Phys., V. 9, 1976, pp.1239-1252, doi:10.1088/0022-3727/9/8/010

[29] King A., Roffle J.F., "Studies on the settlement of hydrating cement suspensions", J. Phys. D: App. Phys., V.9, 1976, pp.1425-1443

[30] Scherer G.W.; Zhang J.; Thomas J. J., "Nucleation and growth models for hydration of cement", Cem. Concr. Res., V.42, 2012, pp.982-993

[31] Perrot A.; Lecompte T.; Khelifi H.; Brumaud C.; Hot J.; Roussel N., ”Yield stress and bleeding of fresh cement pastes”, Cem. Concr. Res., V.42, 2012, pp.937-944

[32] Pierre A., Perrot A., Picandet V., Guevel Y., “Cellulose ethers and cement paste permeability”, Cem. Concr. Res., V.72, 2015, pp.117-127

[33] Radocea A., “A Study on the Mechanism of Plastic Shrinkage of Cement-Based Materials”, PhD thesis, 1992, Chalmers University of Technology

[34] Peng Y., “Sedimentation and bleeding of fresh cement paste”, Doctoral thesis, Norwegian University of Science and Technology, 2014:89 ISBN 978-82-326-0102-8 (printed), 2014:89 ISBN 978-82-326-0103-5 (electronic), 2014, Trondheim, Norway

[35] ASTM C 1679 – 08 “Standard Practice for Measuring Hydration Kinetics of Hydraulic Cementitious Mixtures Using Isothermal Calorimetry”, 2008, 14p

[36] Amziane S., Perrot A. Lecompte T., “A novel settling and structural buildup measurement method”, Meas. Sci. Tech. 2008, V.19, doi:10.1088/0957-0233/19/10/105702

[37] Turbiscan Lab – User Guide, by Formulaction SA, France, 2006Powers T.C., “Properties of Fresh Concrete”, ISBN-13: 978-0471695905 published by Wiley, 1968, 664 p.

[38] Green M.D., Boger D.V., “Yielding of suspensions in compression”. Ind. Eng. Chem. Res., V.36, 1997, pp.4984-4992

[39] Wallevik J. E., “Rheology of particle suspensions: fresh concrete, mortar and cement paste with various types of lignosulfonates”, Doctoral thesis in Norwegian University of Science and Technology, 2003:18 ISBN 82-471-5566-4 (printed), 2003, Trondheim, Norway

[40] Justnes H., Van Gemert A., Sellevold E.J., “Total and external chemical shrinkage of low w/c ratio cement pastes”, Advan. Cem. Res., V.8, 1996, pp.121-126

[41] Tazawa E., Miyazawa S., Kasai T., “Chemical shrinkage and autogeneous shrinkage of cement paste”, Cem. Conc. Res., V.25, 1995, pp.288-292

[42] Hammer T.A.M, Smeplass S., De Weerdt K., Peng Y., “Stability of SCC-robustness for changes in water content and sand grading”, COncrete Innovation Center (COIN) report, 2013, 28p.

Table 1: The recipes of all the samples

No.	Sample code	w/c	solid fraction Φ	lign. type	dosage (sbwc)
1	wc0.4	0.4	0.442	/	/
2	wc0.5	0.5	0.388		
3	wc0.6	0.6	0.346		
4	wc0.7	0.7	0.312		
5	23-wc0.4p0.3	0.4	0.442	DP1523	0.3
6	23-wc0.5p0.3	0.5	0.388		
7	23-wc0.6p0.3	0.6	0.346		
8	23-wc0.5p0.2	0.5	0.388	DP1523	0.2
9	23-wc0.5p0.5				0.5
10	24-wc0.4p0.3	0.4	0.442	DP1524	0.3
11	24-wc0.5p0.3	0.5	0.388		
12	24-wc0.6p0.3	0.6	0.346		
13	24-wc0.4p0.5	0.4	0.442	DP1524	0.5
14	24-wc0.5p0.5	0.5	0.388		
15	24-wc0.4p0.8	0.4	0.442	DP1524	0.8
16	24-wc0.5p0.8	0.5	0.388		
17	24-wc0.6p0.8	0.6	0.346		
18	25-wc0.4p0.3	0.4	0.442	DP1525	0.3
19	25-wc0.5p0.3	0.5	0.388		
20	25-wc0.6p0.3	0.6	0.346		
21	25-wc0.5p0.2	0.5	0.388	DP1525	0.2

22	25-wc0.5p0.5				0.5
23	26-wc0.4p0.3	0.4	0.442	DP1526	0.3
24	26-wc0.5p0.3	0.5	0.388		
25	26-wc0.6p0.3	0.6	0.346		
26	26-wc0.5p0.2	0.5	0.388	DP1526	0.2
27	26-wc0.5p0.5				0.5
28	23-wc0.7p0.3	0.7	0.312	DP1523	0.3
29	24-wc0.7p0.3	0.7	0.312	DP1524	
30	25-wc0.7p0.3	0.7	0.312	DP1525	
31	26-wc0.7p0.3	0.7	0.312	DP1526	

Table 2: The characteristics of four types of lignosulfonate (LS)

Characteristic	DP1523	DP1524	DP1525	DP1526
DM, %	40	40	40	40
Mw	45700	35000	87100	6000
Mn	2650	2650	5100	1250
pH, 10% solution	7.8	4.4	8.2	6.8
Insoluble, w/w %	0.03	0.67	0.01	0.5
Reducing sugars, %	0.8	7.3	<0.5	4.1
Calcium, %	0.4	4.6	0.03	6.6
Sodium, %	8.8	0.4	6.1	0.2
Chloride, %	<0.05	<0.05	<0.05	0.2

Sulphate, %	1.5	0.4	0.5	0.2

Table 3: The characteristics of Portland cement

Composition	SiO_2	Al_2O_3	Fe_2O_3	CaO	MgO	P_2O_5	K_2O	Na_2O	SO_3	Blaine [m^2/kg]	D_{50} [μm]	Specific weight [g/cm^3]
STD-CEM I	20.98%	5.13%	5.13%	60.61%	2.39%	0.14%	0.86%	0.43%	3.01%	382	13.3	3.15

Table 4: all calculated bleeding in fast bleeding period and the first 2 h with parallel measurement results and K-C Eq.

cement paste code	Test method 1: visual bleeding	fast initial bleeding period 1 defined by Turbiscan	Test method 2: Turbiscan			Test method 3: HYSPT			calculated bleeding rate by K-C Eq. (Eq. 1)
	average bleeding rate in 2 h		aver. dh/dt in fast initial period 1 (< nick point)	average dh/dt in dismishing period 2 (nick to 2 h)	Notes	average dh/dt in period 1	average dh/dt in period 2	Notes	
	[m/s]		[m/s]	[m/s]		[m/s]	[m/s]		[m/s]
wc0.7	$1.9 \cdot 10^{-5}$	0.5	$2.0 \cdot 10^{-6}$	$3.0 \cdot 10^{-7}$	calculate from	$7.9 \cdot 10^{-6}$	$2.3 \cdot 10^{-6}$	calculate from top	$4.8 \cdot 10^{-6}$
23-wc0.7p0.3	$2.6 \cdot 10^{-5}$	0.5	$6.4 \cdot 10^{-7}$	$1.8 \cdot 10^{-7}$		$7.8 \cdot 10^{-6}$	$1.4 \cdot 10^{-6}$		

24-wc0.7p0.3	$2.6 \cdot 10^{-5}$	0.5	$1.3 \cdot 10^{-6}$	$1.8 \cdot 10^{-7}$	Turbiscan without oil top setup	$8.1 \cdot 10^{-6}$	$2.9 \cdot 10^{-6}$	pressure	
25-wc0.7p0.3	$3.3 \cdot 10^{-5}$	0.5	$2.2 \cdot 10^{-6}$	$1.5 \cdot 10^{-7}$		$6.9 \cdot 10^{-6}$	$2.5 \cdot 10^{-6}$		
26-wc0.7p0.3	$2.5 \cdot 10^{-5}$	0.5	$2.2 \cdot 10^{-6}$	$1.5 \cdot 10^{-7}$		$6.9 \cdot 10^{-6}$	$2.9 \cdot 10^{-6}$		
wc0.4	/	0.5	$4.5 \cdot 10^{-7}$	$1.6 \cdot 10^{-9}$	calculate from Turbiscan with oil top setup	/	/	calculate from middle pressure	$1.4 \cdot 10^{-6}$
wc0.5	$4.5 \cdot 10^{-6}$	1.0	$6.8 \cdot 10^{-7}$	$1.1 \cdot 10^{-7}$		$9.0 \cdot 10^{-6}$	$5.4 \cdot 10^{-6}$		$2.1 \cdot 10^{-6}$
wc0.6	/	1.0	$9.3 \cdot 10^{-7}$	$7.0 \cdot 10^{-8}$		/	/		$2.9 \cdot 10^{-6}$
wc0.7	$1.9 \cdot 10^{-5}$	0.5	$4.8 \cdot 10^{-6}$	$3.6 \cdot 10^{-7}$		/	/		$3.8 \cdot 10^{-6}$
24-wc0.4p0.3	$1.4 \cdot 10^{-6}$	1.0	$9.5 \cdot 10^{-7}$	$7.0 \cdot 10^{-7}$		$4.8 \cdot 10^{-6}$	$2.9 \cdot 10^{-6}$		$1.4 \cdot 10^{-6}$
24-wc0.4p0.5		/	/	/		/	$3.5 \cdot 10^{-5}$		/
wc0.5	$4.5 \cdot 10^{-6}$	1.0	$6.8 \cdot 10^{-7}$	$1.1 \cdot 10^{-7}$		$9.0 \cdot 10^{-6}$	$5.4 \cdot 10^{-6}$		$2.1 \cdot 10^{-6}$
23-wc0.5p0.3	$2.5 \cdot 10^{-6}$	1.0	$6.1 \cdot 10^{-7}$	$8.2 \cdot 10^{-8}$		$6.5 \cdot 10^{-6}$	$3.2 \cdot 10^{-6}$		$2.1 \cdot 10^{-6}$
24-wc0.5p0.3	$4.3 \cdot 10^{-6}$	1.0	$4.8 \cdot 10^{-7}$	$9.3 \cdot 10^{-8}$		$8.0 \cdot 10^{-6}$	$3.9 \cdot 10^{-6}$		$2.1 \cdot 10^{-6}$
25-wc0.5p0.3	$5.6 \cdot 10^{-6}$	/	/	/		$6.4 \cdot 10^{-6}$	$2.7 \cdot 10^{-6}$		$2.1 \cdot 10^{-6}$
26-wc0.5p0.3	$5.8 \cdot 10^{-6}$	1.0	$8.0 \cdot 10^{-7}$	$1.4 \cdot 10^{-7}$		$5.3 \cdot 10^{-6}$	$3.2 \cdot 10^{-6}$		$2.1 \cdot 10^{-6}$
23-wc0.5p0.5	$4.8 \cdot 10^{-6}$	0.5	0.0	$2.1 \cdot 10^{-7}$		$7.1 \cdot 10^{-7}$	$4.0 \cdot 10^{-7}$		$2.1 \cdot 10^{-6}$
24-wc0.5p0.5	$1.1 \cdot 10^{-7}$	/	/	/		/	$1.0 \cdot 10^{-5}$		$2.1 \cdot 10^{-6}$
25-wc0.5p0.5	$7.2 \cdot 10^{-6}$	/	/	/		/	$2.2 \cdot 10^{-6}$		$2.1 \cdot 10^{-6}$
26-wc0.5p0.5	$1.1 \cdot 10^{-7}$	1.0	$7.3 \cdot 10^{-8}$	$5.9 \cdot 10^{-8}$		$9.0 \cdot 10^{-7}$	$3.3 \cdot 10^{-7}$		$2.1 \cdot 10^{-6}$
23-wc0.6p0.3	/	1.0	$7.3 \cdot 10^{-7}$	$9.3 \cdot 10^{-8}$		/	/		$2.9 \cdot 10^{-6}$
24-wc0.6p0.3	$1.3 \cdot 10^{-5}$	/	/	/		/	$6.0 \cdot 10^{-6}$		$2.9 \cdot 10^{-6}$
26-wc0.6p0.3	/	1.0	$6.4 \cdot 10^{-7}$	$1.2 \cdot 10^{-7}$		/	/		$2.9 \cdot 10^{-6}$